A proper methodology aimed at surface wave tomography

F. Javier Sabadell([1]), **Francisco J. Serón**([2]) **and José Badal**([3])
([1]) *Civil Engineering School, Polytechnic, University of Cataluña, Barcelona, Spain*
([2]) *Department of System Engineering and Computer Sciences, CPS, University of Zaragoza, Zaragoza, Spain*
([3]) *Department of Theoretical Physics and Geophysics, University of Zaragoza, Zaragoza, Spain*

Abstract
When applying a methodology for obtaining the 3D shear-wave velocity structure of a medium from surface wave dispersion data, the problem must be considered with caution since one inverts path-averaged velocities and the use of any inversion method entails some drawbacks such as lack of uniqueness, unwarranted stability and constraints affecting the data. In order to avoid the application of consecutive inversions and to overcome these drawbacks, we propose alternative mapping methods, for example spatial prediction methods, or else the use of an algorithm that, from a mathematical viewpoint, can be understood through the application of the orthogonal projection theorem onto convex sets (POCS). Among the first ones, we try inverse weighted distance interpolation. The POCS algorithm we have used discretises a second order differential equation for the velocity field with boundary conditions. All these imaging techniques aimed at volumetric modelling and the visualisation of data are discussed, and finally we show some results based on ray path velocities obtained previously by inversion of phase and group velocities of Rayleigh waves propagating across the Iberian peninsula.

Key words *Iberian peninsula – gridding techniques – POCS algorithm – tomographic images*

1. Introduction

As is common practice when studying surface wave propagation and inverting velocity dispersion curves in order to obtain Earth models, the data are ray path phase and group velocities determined by digital filtering, which are then inverted on the basis of the inverse theory to obtain shear-wave velocity profiles (Badal *et al.*, 1990, 1992). Inverse modelling results in 1D models necessarily referred to the paths travelled by the waves, and the shear velocity variation with depth is normally defined for a layered medium in terms of average values per layer.

An alternative method for the analysis and quantitative interpretation of surface-wave dispersion data has recently been proposed by Nikolova *et al.* (1997), consisting in: a) a previous regionalization of the observed ray path phase and group velocities of surface waves; b) construction of velocities independently of the paths at a set of points over the region; c) inversion for local velocity structure. For the purpose of regionalization of velocities, a procedure based on the Backus-Gilbert method for linear inversion of travel times of surface waves (Yanovskaya, 1984; Gobarenko *et al.*, 1987; Yanovskaya *et al.*, 1988, 1990), which leads to a continuous function representing the velocity distribution over the area covered by ray paths, was used. Linear inversion of travel

Mailing address: Dr. F. Javier Sabadell, Civil Engineering School, Polytechnic, University of Cataluña, Gran Capitán, 08034 Barcelona, Spain; e-mail: javier@zar.unizar.es

time data yielded phase and group velocity contour maps for several reference periods. After constructing local dispersion curves at different grid points over the region the curves were inverted using an inversion procedure based on the inverse theory (Menke, 1984; Parker, 1994; Tarantola, 1987) for local shear-wave velocity structure.

Such a working scheme provides velocity-depth functions at a set of points independently of the paths, and the construction of interpolated shear velocity patterns from them is straightforward. Any dependence of the phase and group velocity on the ray path, which is the usual case, is avoided, and joint inversion of phase and group velocities for local velocity structure is possible. The method has the advantage that no *a priori* division of the investigated region into blocks is necessary, *i.e.* it does not require a subjective choice of boundaries, and thus the results are not affected by regionalization. However, the method proposed involves two consecutive inversion processes: first, to determine regionalised or local surface-wave velocities; second, to invert regionalised or local dispersion curves before mapping to obtain a volumetric model. In this point the difficulty arises from the use of an inversion method twice, since any inversion method entails some drawbacks such as lack of uniqueness, unwarranted stability and constraints affecting the data.

From a mathematical viewpoint, in surface wave tomography we meet a classic inversion problem in which the data are linear functionals of the model and the equation for the model is a Fredholm integral equation of the first kind. In effect, a perturbation in phase velocity C along the i-th path can be expressed as the average

$$\delta C_i(\omega) = \frac{1}{L_i} \int_L \delta C(\omega, \theta, \phi)\, dl \qquad (1.1)$$

where $\delta C(\omega, \theta, \phi)$ are the local perturbations on that path and L is its length. In this expression the phase velocity C can be replaced by the group velocity U, both depending on the frequency ω. If we assume that a perturbation $\delta\beta$ in shear velocity, which depends on depth z, leads to a variation δC in phase velocity, we have

$$\delta C(\omega, \theta, \phi) = \int_0^\infty \left[\frac{\delta C}{\delta \beta}\right]_{\omega, z} \delta\beta(\theta, \phi, z)\, dz. \qquad (1.2)$$

Substituting (1.2) in (1.1), we obtain the integral

$$\delta C_i(\omega) = \frac{1}{L_i} \int_L \int_0^\infty \left[\frac{\delta C}{\delta \beta}\right]_{\omega, z} \delta\beta(\theta, \phi, z)\, dz\, dl. \qquad (1.3)$$

This expression poses a classic inversion problem which in its more general form can be formulated as

$$d(\boldsymbol{x}) = \int_\Omega G(\boldsymbol{x}, \boldsymbol{y})\, m(\boldsymbol{y})\, d\boldsymbol{y} \qquad (1.4)$$

where $G(x, y)$ are the data kernels, d represents the data vector and m the model vector. If there is no trivial solution $a(y)$ to

$$0 = \int_\Omega G(\boldsymbol{x}, \boldsymbol{y})\, a(\boldsymbol{y})\, d\boldsymbol{y} \qquad (1.5)$$

then the solution of the tomographic experiment is unique. In the physical processes of our interest the uniqueness of the solution can seldom be established. A way to overcome this difficulty consists of transforming the equation (1.5) by means of one of the well studied integral transforms (Laplace, Fourier, Hankel, Volterra, ...).

2. Spatial prediction methods

Since our interest is to study lateral distributions of velocity patterns on the Iberian peninsula, and due to the difficulties arising from successive inversion problems, firstly we propose to apply alternative methodologies based on mathematical gridding algorithms. These methods (which can be considered as simple interpolation schemes) are efficient and easy to implement, and ease the following facilities: a) solution constrained according to initial (or

experimental) data; b) information visualised throughout a graphic display of the data; c) representation illustrated by a surface or a volume.

Several techniques may be used to produce such information. Gridding can be viewed as an operator that maps the data $(x_i, y_i, z_i; F_i)$ to the trivariate function $F(x, y, z)$ over a grid. For some applications, a suitable function F must be chosen carefully, being a crucial point for the entire process. But, given the characteristics of our problem, the imaging process in itself and the way we obtain valuable results are more important than the form of the mapping function. We describe some methods below. In the final part, we apply one weighted distance method to our data.

2.1. *Fitting of local trend surfaces*

The simplest way to describe gradual variations of a property is to model them by polynomial regression. The idea is to fit a polynomial surface by least squares through the data points. Let us assume that the spatial coordinates X and Y are the independent variables, and that Z (the property of interest) is the dependent variable. In two dimensions the polynomials are surfaces of the form:

$$Z(X, Y) = \sum_{r+s \leq p} (b_{rs} X^r Y^s) \qquad (2.1)$$

where r and s are the polynomial coefficients, p is the order of the trend surface and b_{rs} is a constant. Two major disadvantages of this general trend analysis are the susceptibility to outliers and the inability to fit a low order polynomial through complex data. However, they can be reduced with a moving window approach (Leenaers *et al.*, 1990).

2.2. *Kriging*

Kriging is a distance weighting, moving average estimation method where optimal weights are obtained from a graph (variogram) of scattered data (Krajewski and Gibbs, 1996). With this approach, kriging becomes a «geostatistical» method, *i.e.*, a statistical method that is applied in such a way to take into account what is known about the spatial characteristics of the parameters involved. When the variogram is well behaved and well known, the resulting kriged estimate is frequently stated to be the best, linear, unbiased estimate (BLUE) that can be calculated. Once the variogram is modelled and its descriptive parameters determined, kriging estimation can begin. This is accomplished by solving a system of simultaneous, linear equations. More specifically, the solution consists of calculating the weights that should be given to surrounding data values to minimise the error of the estimate at each cell node. Kriged results provide a solution where the mean squared error at each cell node equals zero. This differs from inverse distance weighting where each scattered data points weight is computed separately as a function of the geographic distance between scattered data points and cell node locations, and the sum of all distances between scattered data points and cell node locations. In spite of the clear advantages mentioned above, this method is very sensitive to the number of data points: the amount of calculation time increases as this number increases. In our case, we process large data sets which become this method low-efficient. In addition, time is needed to understand a site-specific variogram and to construct a reliable variogram that fits the spatial variation of the parameter being investigated. Nevertheless, it is a powerful tool currently under study that we are trying to implement.

2.3. *Distance function approach*

Given a set of data points, one of the simplest mathematical expression for a continuous surface that intersects these points is an interpolating polynomial that passes through all data points. The linearity of the process implies that the modelling function can be represented as combination of some basis. The cubic spline basis, that is, the solution obtained when the energy function is minimised, is a useful choice. This results in the smoothest function which passes through the data. Given the data

(x_i, F_i), the cubic spline representation F is characterised by the following conditions:

– F, F' and F'' are continuous;

– $F(x_i) = F_i$;

– F is piecewise cubic, that is, on each interval $[x_i, x_{i+1}]$ is a cubic polynomial;

– F is linear on the extreme of the data interval.

The straightforward equation of this approach is as follows:

$$F(p) = \sum_{i=1}^{N} c_i \|p - p_i\|^3 + a + bx + cy + dz \quad (2.2)$$

where $p = (x, y, z)$ and $p_i = (x_i, y_i, z_i)$. Imposing the four conditions just mentioned, we calculate the coefficients by solving the system of equations:

$$\begin{bmatrix} |p_i - p_j|^3 & \cdots & \cdots & 1 & p_1 \\ \vdots & \ddots & & 1 & p_2 \\ \vdots & & \ddots & 1 & p_N \\ 1 & 1 & 1 & 0 & 0 \\ p_1^t & p_2^t & p_N^t & 0 & 0 \end{bmatrix} \begin{bmatrix} c_1 \\ c_2 \\ \vdots \\ c_N \\ a \\ b \\ c \\ d \end{bmatrix} = \begin{bmatrix} F_1 \\ F_2 \\ \vdots \\ F_N \\ 0 \\ 0 \\ 0 \\ 0 \end{bmatrix} \quad (2.3)$$

When the number of data points is very large, then methods based upon distance functions may not be a practical way of modelling. In fact, distance function methods require to solve *for every point* a linear system of equations of the size $(N+4)\times(N+4)$ where N is the number of data points. Moreover, these systems can be very badly conditioned.

2.4. *Inverse Weighted Distance (IWD) interpolation*

The principle upon which the distance weighting methods are based on, is to assign more weight to nearby points than to distant points. The idea is that observations located close together tend to be more alike than observations spaced further apart. The most common form for the values to be estimated is:

$$Z(x_j) = \frac{\sum_{i=1}^{n} Z(x_i)\, d_{ij}^{-W}}{\sum_{i=1}^{n} d_{ij}^{-W}} \quad (2.4)$$

where x_j is the point at which the surface is to be interpolated, x_i is a data point, d_{ij} is the interdistance and W is the weighting exponent. For $d = 0$ the exact value of the original sample has to be preserved. The factors controlling the results include the following items:

– *The weighting exponent.* By changing the exponent, the distribution of scattered data point weights can be from highly biased in favor of the nearest data points, to nearly equal for all data points. The greater the exponent, the more detailed and less smoothed the results are.

– *The search area size and the number of data points.* In general, the use of small search areas and few scattered data points results in the «enhancement» of local anomalies since few data are being averaged. Conversely, the use of large search areas and many scattered data points results in the «smoothing» of local anomalies since many data are being averaged. Scattered data points should come from different locations surrounding the cell node. If these data are clustered to one side of the cell node and are used, then the estimated cell node value may be biased. In such a case, a new definition of the weight should be adopted (Weber and Englund, 1992).

There are several disadvantages to take into account: first, the choice of a weighting function may introduce ambiguity; second, the method is easily affected by uneven distribution of data points; third, the method is, by definition, a smoothing technique, that is, maxima and minima in the interpolated surface can occur only at data points. Therefore, the location and values of extremes cannot be detected when they are not included as original samples.

2.5. *Results*

We have applied this last interpolation technique by considering as starting data the inver-

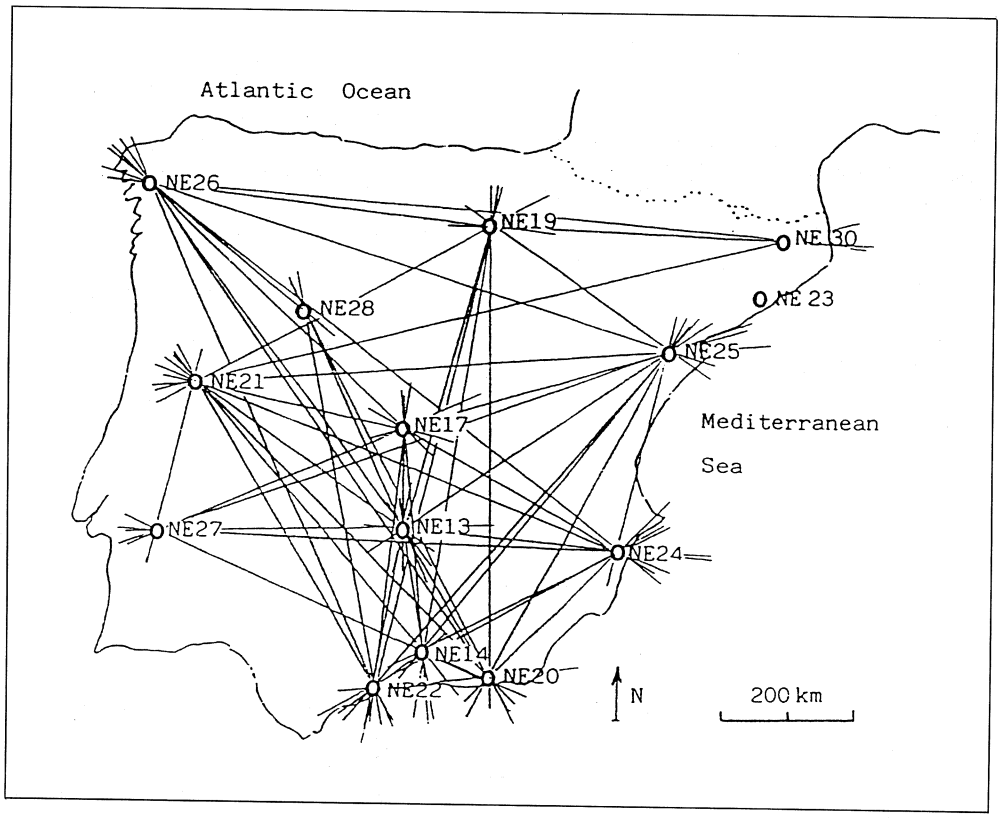

Fig. 1. ILIHA array in the Iberian peninsula (station NE23 was moved to NE30). The path coverage for two-station surface wave velocity measurements is displayed by straight lines which represents approach directions of the wave fronts crossing the Iberian area.

sion results obtained from the high-quality long-period data recorded at broadband stations installed in the Iberian peninsula during the ILIHA broadband seismology experiment (details are given in Appendix).

As the resolution kernels associated with the layered model are found to be narrow in width for the upper 200 km, the total depth interval of reliability is approximately 20-200 km. Unfortunately, the first 20 km of the crust are not well defined for the range of periods used. Of course, the wavelengths longer than 30 km (periods greater than 10 s) that we use do not account for the results obtained via generalised inversion for the top crustal layers. This part of the layered model is an underresolved region needed as part of the inversion process but having only limited physical significance. The fine structure at shallow depths is certainly not resolved, but this fact does not detract from our study, since its major results concern the mantle.

We sampled each trajectory with a number of equidistant data points, three per path, which results in an irregular grid covering the global domain, as the paths travelled by the waves are not homogeneously distributed (fig. 1). The pathwise restriction we want to preserve is already done with the mentioned process. The irregular grid so obtained can be firstly viewed as a disadvantage; however,

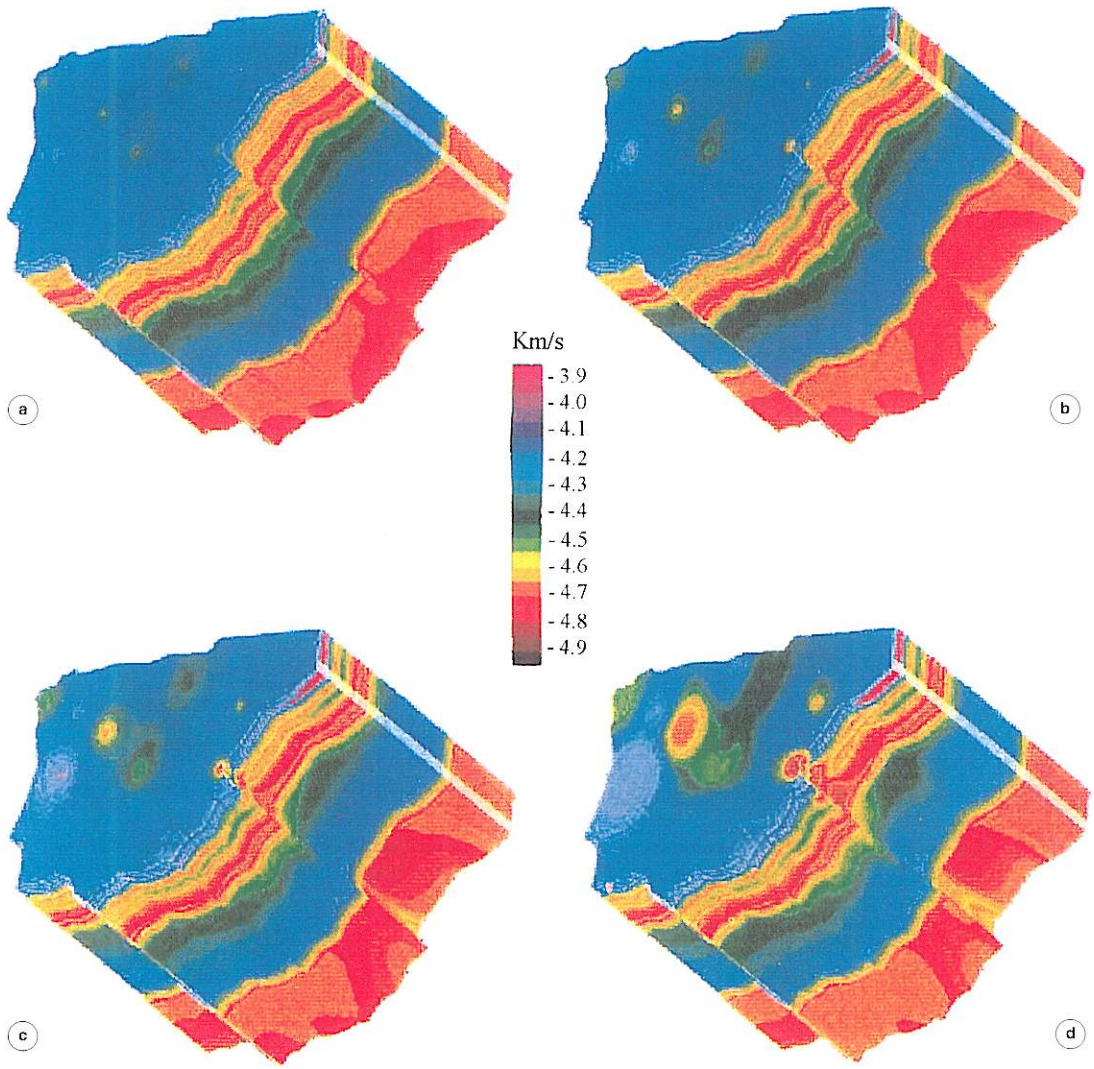

Fig. 2a-d. Volumetric views of the Iberian peninsula showing its seismic velocity structure obtained using IWD interpolation. Each structure corresponds to a different value of the exponent in the weighting function: a) 0.5; b) 1.5; c) 2.0; d) 4.0. In the pictures, blue tones correspond to the lower velocity values, and red or yellow tones correspond to the higher ones.

since we are not interested in a smooth velocity field, the use of such a grid and of a proper weighting exponent enhances the local properties of the seismic velocities.

Figure 2 a-d shows four different volumetric representations according to four different exponent values: 0.5, 1.5, 2.0 and 4.0. The process to construct the 3D images involves a voxel technique that permits us to display a solid volume under different viewpoints (rota-

tion) and different features (level of invisibility for a selected range of colours, cutting by different planes, user-applied source light, brilliance and contrast levels, etc.). The volume is constructed by linear interpolation of the different reference layers obtained by the IWD approach, in order not to introduce spurious information. We must point ont that colours are not equivalent in the pictures, but they are very similar. Low exponents tend to smooth data, which means that they badly reach maxima and minima. High exponents tend to emphasize the extremes better. Therefore, the velocity intervals (palettes of colour) are not *exactly* the same.

Results obtained applying the lowest exponents are highly biased in favor of average values per layer (fig. 2a,b). As the exponent increases, distinct structures start to appear with each layer (fig. 2c,d), which means that the variability in the property under study, between data point locations, is more accurately displayed. As expected, the vertical heterogeneity is very similar for the cases in which we choose a lower exponent. A relatively high exponent (for example 4.0) displays not only the lateral variations supplied by the data, but also the vertically heterogeneous structure.

3. Method of projections onto convex sets

The main drawback of any of the methods described in the last section is that none of them guarantees the absence of velocity fluctuations between two points belonging to the same trajectory. This led us to propose another method of volumetric reconstruction based on the orthogonal projection theorem for convex sets, which yields more accurate solutions for path-averaged data and is well aimed to volumetric reconstruction of dispersion results. As we will see later, this tecnique is a different approach to inverse problems, carried out by iteration.

As is well known, a set of possible underlying (or images) $\{u\}$ is said to be convex if for any two elements in the set all the interpolated combinations are also in the set:

$$(1-\nu)u_a+\nu\, u_b \in \{u\},$$

$$\forall u_a,\, u_b \in \{u\}, \qquad 0 \le \nu \le 1. \qquad (3.1)$$

Many deterministic constraints that one might want to impose on the solution u of an inverse problem, in fact define convex sets; for example, positivity of the solution ($u \ge 0$), compact support ($u(x) = 0$ outside of a certain region), or known bounds ($u_L(x) \le u(x) \le u_U(x)$ for specified upper (u_U) and lower (u_L) bounds) that may be connected with an initial estimate of the solution: $u_0(x) \pm \gamma\sigma(x)$. These and other restrictions can be accomplished either in the image space or in the space given by any linear transformation of u.

On the assumption that C_i is a convex set, $\mathcal{P}_i$ is called a nonexpansive projection operator onto the set if: i) $\mathcal{P}_i$ leaves unchanged any element already in C_i, and ii) $\mathcal{P}_i$ maps any element $\hat{u}$ outside C_i to the closest element of C_i, in the sense that

$$|\, \mathcal{P}_i\, \hat{u} - \hat{u}\,| \le |\, u_a - \hat{u}\,| \quad \forall u_a \in C_i. \qquad (3.2)$$

This definition sounds complicated, but examples of such operators are quite simple. A nonexpansive projection onto the set of positive u's is: a) set all negative components of u equal zero; b) set zero the values outside the region support; c) set all values less than a lower bound equal to that lower bound and set all the values greater than an upper bound equal to that upper bound. The usefulness of these definitions consists in the following theorem:

– Theorem: let C be the intersection of m convex sets C_1, C_2, C_3, C_4, ..., C_m. Then the iteration

$$u^{(k+1)} = (\mathcal{P}_1\, \mathcal{P}_2 \ldots \mathcal{P}_m)\, u^{(k)} \qquad (3.3)$$

will converge to C from all starting points as $k \to \infty$. If C is empty (there is no intersection), then the iteration will have no limit point.

The application of this theorem is called the *method of projections onto convex sets* or sometimes POCS by its acronym (Biemond *et al.*, 1990). We can generalise by replacing any operator $\mathcal{P}_i$ by

$$\mathcal{T}_i \sim 1+\beta_i(\mathcal{P}_i-1), \quad 0 < \beta_i < 2. \quad (3.4)$$

An adequate choice of the parameters β_i allows to increase the convergence.

It is to be noted that some inverse problems can be completely solved by iteration alone. It is a question of determining the solution through a POCS algorithm. In our case and operating with seismic wave velocities, the method is equivalent to projecting iteratively the velocity image onto the set of all such images that satisfy Laplace's equation and the set of all such images that have the observed path-averaged layer velocities. As such, its convergence properties can be understood through application of the orthogonal projection theorem for convex sets. This is equivalent to discretising the following boundary condition problem referred to inverted (shear wave) velocities:

$$\Delta u = 0, \qquad \forall u \in \Omega \quad (3.5)$$

$$u_{|\Gamma i} = \bar{u}_i;$$

$$u_0 = \bar{u}$$

where Ω represents the domain in which the velocities to be interpolated are defined (a surface at a reference depth); Γ_i is the great circle path corresponding to the i-th trajectory; u_i is the path-averaged velocity for the i-th trajectory; and u_0 is the initial velocity value adopted to start the process, which is taken as the mean velocity at a reference depth.

3.1. *The algorithm*

We use a particular method of mapping, according to an iterative method based on Laplacian interpolation, for obtaining a 3D picture of the Iberian continental domain. As before, our starting data are path-averaged shear wave velocities at different depth intervals (Badal *et al.*, 1996), and we want to interpolate these ray path velocity values to a volume represented by discrete cubic elements (voxels) each with a particular velocity value.

The first step is to construct a matrix having grid point velocity values as elements for each top layer depth where we have only ray path velocity data. This can be made by assigning grid points to the locations of the stations by means of a single transformation of coordinates and a single velocity value along each seismic path. A mean value can be assigned in the intersection of two paths. Next, the other elements of the matrix can be defined taking an initial velocity value for all them. We take as initial velocity the (constant) averaged velocity data for all the paths. These operations do not restrict the generality of the procedure at this step of beginning of the procedure.

The second step consists of the calculation of new velocity values for each reference depth by means of a linear interpolation algorithm like Laplacian interpolation. As is well known, this algorithm involves four values in the calculation of a particular velocity. Likewise, it can be extended without difficulty to the determination of velocities in the border of the grid. Of course, there is no problem in using another type of interpolation. After this, it is obvious that various velocities emerge instead of the constant velocity corresponding to a two-station velocity estimate, which results very probably in a mean value different from the observed one. However, the Earth models obtained by inversion, and consequently the distributions of path-averaged shear wave velocity at different depth intervals, are the only available information that we have to try a 3D picture. Therefore we must recover the previous two-station velocity measurements.

The third step of the process consists in the restitution only of the velocities supplied by inversion for all the seismic trajectories studied. This task is very simple and can be carried out by readjusting only those elements of the matrix involved by a proper factor of conversion. Small differences in the averaged-path velocities can appear due to rounding-off errors and

the application of two distinct factors in the points where two paths pass each other, but these differences are practically negligible (close to zero). The procedure is restarted, and the solution can be obtained by successive iterations. The procedure is repeated until the differences in velocity converge to a solution which reduces the residuals to a satisfactory minimum (less than 1.0%).

In summary, the iterative method applied here generates different velocity values along the trajectory travelled by the waves between two stations, though the mean velocity is always kept equal to the previously determined ray path velocity. The method allows one to obtain interpolated velocity values in such a way that there are no jumps in the cutoff points between seismic paths, the seismic wave velocities varying with smoothness.

Once the matrices have been calculated at particular depths, the next and last step is to compute the data planes which make up the 3D data matrix for the real volume that we use for 3D representation. Each one of these reference horizontal planes is between two nearby matrices, one above and one below. Finally, the data upon these planes which are uniformly distributed along the total depth of the Earth structure can directly be calculated by linear interpolation by considering the respective above and below matrices. Figure 3 shows a flowchart of this volumetric visualisation algorithm.

3.2. *Results*

The 3D mapping of shear wave velocity that we have performed, which is based on the method explained above, allows us to obtain tomographic images of the subcrustal lithosphere and asthenosphere of Iberia. As before,

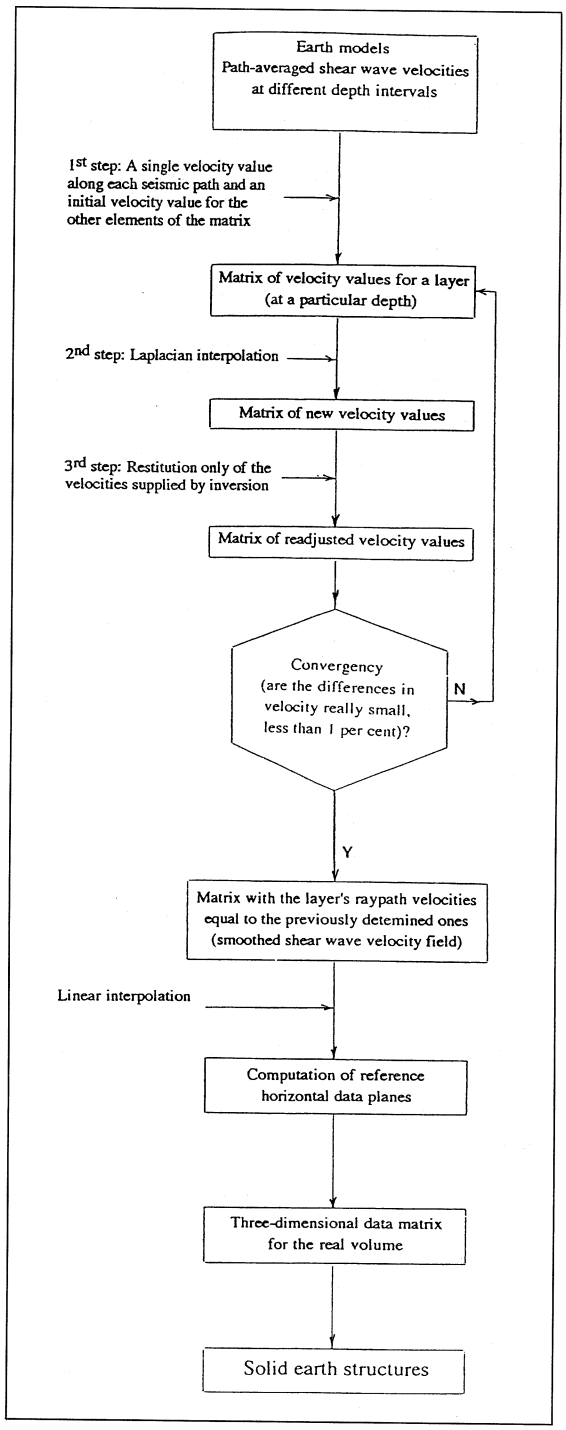

Fig. 3. Flowchart of the POCS algorithm used in this work for 3D visualisation.

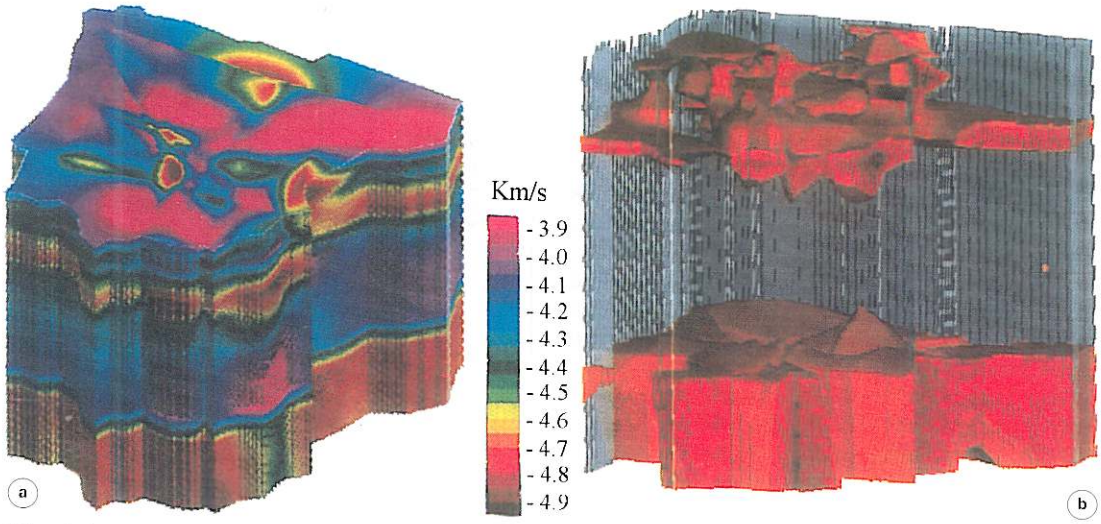

Fig. 4a,b. An overall view of the deep velocity structure of the Iberian peninsula (a) and one image as defined by a characteristic shear wave velocity range, 4.65-4.85 km s^{-1}, which represents the highest shear velocities in the lithosperic mantle and in the upper mantle under the asthenosphere (b). This last structure is solid for velocity values belonging to the prefixed interval and transparent for any values outside this interval.

the outputs can be shown as coloured solid structures in the form of 3D blocks. Thus, a sequence of horizontal slices at gradually increasing and characteristic depths, cross-sections and 3D structures which are solid for velocity values belonging to prefixed intervals and transparent for any values outside these intervals, can be displayed in order to emphasize various patterns. Some details of computation are mentioned as follows. Any square matrix calculated by Laplacian interpolation contains 62500 grid point velocity values. There are 150 reference horizontal data planes which are built by linear interpolation from as many matrices previously determined as information at depths of reference we have. If so, the total number of elements (voxels) of the 3D data matrix, which is representative of the seismic velocity field in the real volume, exceeds 9×10^6 elements (exactly $250\times250\times250$).

Figure 4a,b shows two examples of the results obtained using the POCS algorithm proposed here. The main difference with respect to results obtained with the IWD algorithm is the distinction between images at the same reference depth. The imposition of a hard restriction in order to preserve the path-average velocity value along each path, results in models with strong variations in velocity due to the velocity restitution process named as the third step of the mapping method. The border effects are now clear in comparison with those obtained with IWD interpolation giving rise to sharply contrasting lateral heterogeneity as a consequence of the irregular path coverage (northern peninsular third). Of course, this type of anomalies can be removed or better smoothed afterwards by a smoothing technique applied to the results obtained from the volumetric reconstruction.

4. Concluding remarks

– IWD approach is especially useful for analyzing short range variability between scattered data points. The technique is easy to understand mathematically, requires short calculation times and is a tool which gives reliable values. For all these reasons, it can be considered a good estimator and can be used to «test» ideas.

– POCS algorithm generates an unique estimated surface since a partial differential equation with boundary conditions is satisfied. However, those boundary conditions may cause artifacts, such as edge effects. The estimate is independent of the data distribution. The irregular pattern of data points may cause lack of homogeneous convergency over the global domain.

– The methods of mapping can be applied to both deep velocity structure and near-surface velocity structure in order to highlight large-scale or small-scale features of the structure.

Acknowledgements

The authors acknowledge the helpful comments and suggestions made by Dr. Bruno Alessandrini. This research was partially supported by the Comisión Interministerial de Ciencia y Tecnología (CICYT) under contracts TIC95-0614-C03-01 and MAR95-1916-C02-02, and by the Comissionat per a Universitats i Recerca (Generalitat de Catalunya) through a research grant given to one of the authors (F.J. Sabadell).

REFERENCES

AKI, K. and P.G. RICHARDS (1980): *Quantitative Seismology: Theory and Methods* (W.H. Freeman, New York), vol. II, 675-717.

AL-KHATIB, H.H. and B.J. MITCHELL (1991): Upper mantle anelasticity and tectonic evolution of the Western United States from surface wave attenuation, *J. Geophys. Res.*, **96** (18), 129-146.

BADAL, J., V. CORCHETE, G. PAYO, J.A. CANAS, L. PUJADES and F.J. SERÓN (1990): Processing and inversion of long-period surface-wave data collected in the Iberian peninsula, *Geophys. J. Int.*, **100**, 193-202.

BADAL, J., V. CORCHETE, G. PAYO, F.J. SERÓN, J.A. CANAS and L. PUJADES (1992): Deep structure of the Iberian peninsula determined by Rayleigh wave velocity inversion, *Geophys. J. Int.*, **108**, 71-88.

BADAL, J., V. CORCHETE, G. PAYO, J.A. CANAS and L. PUJADES (1993): Shear wave velocity structure below the Iberian peninsula as obtained by a detailed analysis of surface waves, *Tectonophysics*, **225**, 167-190.

BADAL, J., V. CORCHETE, G. PAYO, L. PUJADES and J.A. CANAS (1996): Imaging of shear wave velocity structure beneath Iberia, *Geophys J. Int.*, **124**, 591-611.

BANDA, E., E. SURIÑACH, A. APARICIO, J. SIERRA and E. RUIZ DE LA PARTE (1981): Crust and upper mantle structure of the Central Iberian Meseta (Spain), *Geophys. J. R. Astron. Soc.*, **67**, 779-789.

BIEMOND, J., R.L. LAGENDIJK and R.M. MERSEREAU (1990): *Proceedings of the IEEE*, **78**, 856-883.

CARA, M. (1973): Filtering of dispersed wavetrains, *Geophys. J. R. Astron. Soc.*, **33**, 65-80.

DZIEWONSKI, A.M., S. BLOCH and M. LANDISMAN (1969): A technique for the analysis of transient seismic signals, *Bull. Seism. Soc. Am.*, **59**, 427-444.

GOBARENKO, V.S., S.B. NIKOLOVA and T.B. YANOVSKAYA (1987): 2D and 3D velocity pattern in Southeastern Europe, Asia Minor and the Eastern Mediterranean from seismological data, *Geophys. J. R. Astron. Soc.*, **90**, 473-484.

HWANG, H.J. and B.J. MITCHELL (1986): Interstation surface wave analysis by frequency-domain Wiener deconvolution and modal isolation, *Bull. Seismol. Soc. Am.*, **76**, 847-864.

KRAJEWSKI, S.A. and B.L. GIBBS (1996): *Understanding Contouring* (Gibbs Associates, Boulder, Colorado), pp. 74.

LEENAERS, H., J.P. OKX AND P.A. BURROUGH (1990): Comparison of spatial prediction methods for mapping floodplain soil pollution, *CATENA*, **6**, 535-550.

MENKE, W. (1984): *Geophysical Data Analysis: Discrete Inverse Theory* (Academic Press, Orlando, Florida) pp. 260.

NIKOLOVA, S.B., J. BADAL and G. PAYO (1997: Local Rayleigh wave velocity dispersion in the Iberian region, *Geophys. J. Int.* (submitted).

NOLET, G., B. DOST and H. PAULSSEN (1985): Intermediate wavelength seismology and the NARS experiment, *Ann. Geophys.*, **4**, 305-314.

PARKER, R.L. (1994): *Geophysical Inverse Theory* (Princeton University Press, Princeton, New Jersey).

PAULSSEN, H. (1990): The Iberian peninsula and the ILIHA project, *Terra Nova*, **2**, 429-435.

PAYO, G. (1970): Structure of the crust and upper mantle in the Iberian shield by means of a long period triangular array, *Geophys. J. R. Astron. Soc.*, **20**, 493-508.

TARANTOLA, A. (1987): *Inverse Problem Theory. Methods for Data Fitting and Model Parameter Estimation* (Elsevier, Amsterdam), pp. 613.

YANOVSKAYA, T.B. (1984): Solution of the inverse problem of seismology for laterally inhomogeneous media, *Geophys. J. R. Astr. Soc.*, **79**, 293-304.

YANOVSKAYA, T.B., R. MAAZ, P.G. DITMAR and H. NEUNHOEFER (1988): A method for joint interpretation of the phase and group surface wave velocities for estimation of lateral variations of the Earth's structure, *Phys. Earth Planet. Inter.*, **51**, 59-67.

YANOVSKAYA, T.B., G.F. PANZA, P.G. DITMAR, P. SUHADOLC and S.T. MUELLER (1990): Structural heterogeneity and anisotropy based on 2D phase velocity patterns of Rayleigh waves in Western Europe, *Rend. Fis. Acc. Lincei*, **9**, 127-135.

WEBER, D. and E. ENGLUND (1992): Evaluation and comparison of spatial interpolators, *Mathematical Geology*, **4**, 381-391.

Appendix. Data and dispersion methodology.

The Iberian Lithosphere Heterogeneity and Anisotropy (ILIHA) project was aimed at increasing the knowledge of the Iberian peninsula lithosphere and asthenosphere structure by means of seismological studies. The ILIHA project contributed in this way to the European Geotraverse (EGT) project, which had as its main objective the investigation of the nature, dynamics, and evolution of the continental lithospere beneath Europe. As part of the ILIHA project (Paulssen, 1990), 13 broadband stations of the portable Network of Autonomously Recording Stations (NARS) (Nolet *et al.*, 1985) were installed in Spain and Portugal. Most of these stations operated for one year (February 1988 to March 1989) and recorded body and surface waves generated by distant and local earthquakes. The installation of the ILIHA array in Iberia provided a large set of digital data and substantially increased the path coverage for two-station Rayleigh wave dispersion measurements.

Starting from ILIHA data sets, we recently performed several dispersion analyses of Rayleigh waves propagating across the Iberian peninsula (Badal *et al.*, 1992, 1993). While off-azimuth arrivals are known to cause bias in dispersion curve estimates, first of all we applied methods to test whether the observed wave fields arrive in the great circle direction to minimise errors due to multipathing effects (Al-Khatib and Mitchell, 1991). We evaluated the accuracy of this approximation for our particular data set and found no significant (< 2°) departures from the expected great circle. In any case, from ILIHA data in the 20-100 s period range, it emerges that the relative error in the value of the phase velocity is less than 1% when calculating path-averaged phase velocities ignoring the deviation of the arrival of the wave from the great circle direction. Figure 1 shows the geographical locations of the NE (NARS Europe) stations on a map of the Iberian peninsula. We found 64 events which met our criteria and were well recorded at two stations. Epicentral locations of these earthquakes correspond to different source regions (fig. 5). Because of the lack of useful data for some of them, a total of 53 pairs of stations was used.

As far as the methods to minimise errors due to higher-mode interference (modal contamination) are concerned, we used moving-window analysis on the signal to obtain approximate group times and then carried out a correction of the waveform using a time-variable filter (Cara, 1973) in order to measure with least possible bias the dispersion of the wavetrain (Badal *et al.*, 1990; Badal *et al.*, 1992). After isolating the fundamental mode from Rayleigh wave trains, we used the multiple filter technique (Dziewonski *et al.*, 1969) to obtain group velocity dispersion. The determination of phase velocity dispersion was performed by applying the stan-

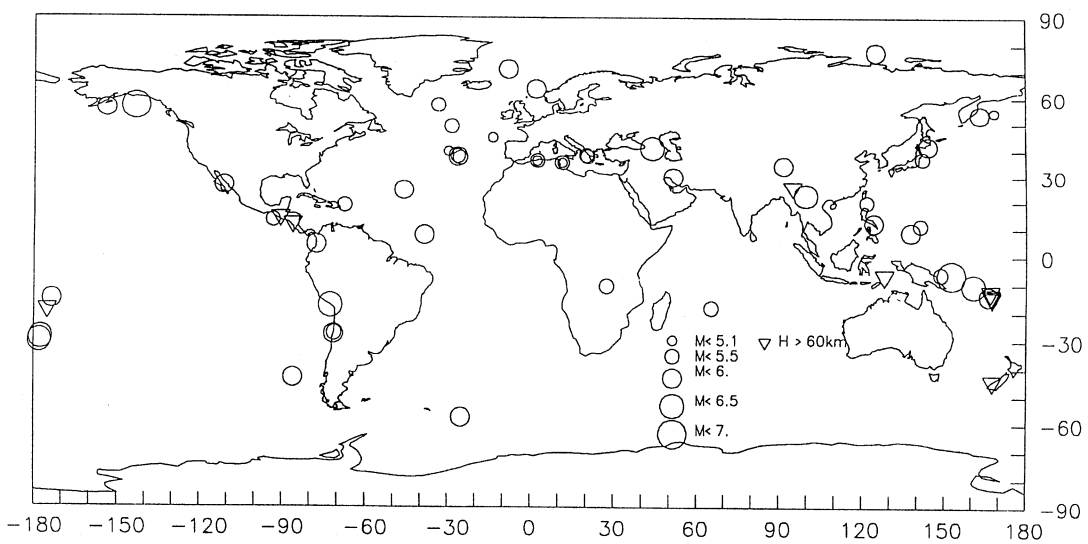

Fig. 5. Epicentral locations of the seismic events used in this study.

dard frequency-domain Wiener deconvolution (Hwang and Mitchell, 1986). We simultaneously inverted phase and group velocities in order to place tighter constraints on possible models (Al-Khatib and Mitchell, 1991). We performed inverse modelling by stochastic inversion (Aki and Richards, 1980) for the determination of the theoretical shear wave velocity models according to the generalised inversion theory (Menke, 1984; Tarantola, 1987). Details of this stochastic inversion approach were given by Badel *et al.* (1992). Such an inversion method requires a proper initial Earth model. To build up the starting Earth model, we considered the *P* and *S* velocity-depth functions as derived from travel time and amplitude interpretations for the crust by Banda *et al.* (1981) and the Iberian (IBE) model based on surface wave dispersion measurements for the upper mantle by Payo (1970).

We estimated the reliability of the inversion results using different methods; first, by calculating the resolving kernels at various reference depths for each solution obtained by the generalised inversion approach; second, by means of forward modelling and comparing solutions of forward problems in terms of phase and group velocity dispersion curves predicted by the respective Earth model obtained by inversion, with the determined dispersion data. A good agreement does not necessarily ensure the uniqueness of the results, but it does indicate that the models obtained from inversions agree well with the velocity measurements. In all cases, inversions were redone by considering the nonuniqueness of the solution and possible effects of *a priori* model parameters. Unrealistic or poorly defined solutions were rejected.

The velocities supplied by linear inversion for all the seismic trajectories studied here are path-averaged shear wave velocities at different depth intervals. The inversion results obtained for each of the 53 paths analysed are shear wave velocity distributions with depth (Badal *et al.*, 1996). Velocity uncertainties are less than 1.4%. This uncertainty figure refers to the maximum uncertainty of any of the velocities per layer, and is a 1σ value.